

THE DORSA ARGENTEA, MARS: COMPARISON TO >5900 TERRESTRIAL ESKER SYSTEMS AND STATISTICAL TESTS FOR TOPOGRAPHIC RELATIONSHIPS. F. E. G. Butcher¹, S. J. Conway^{1,2}, N. S. Arnold³ and Balme, M. R.¹ ¹Department of Physical Sciences, The Open University, Walton Hall, Milton Keynes, MK7 6AA, UK (frances.butcher@open.ac.uk), ² LPG Nantes – UMR CNRS 6112, Université de Nantes, France, ³Department of Geography, University of Cambridge, Downing Place, Cambridge, CB2 3EN, UK.

Introduction: We undertake the first large-scale quantitative analysis of the plan view geometries of the Dorsa Argentea [1] in a comparison to >5900 terrestrial esker systems in Canada [2]. Statistical tests for esker-like topographic relationships [1,3-4,5-6] are also completed. The Dorsa Argentea (DA) are an assemblage of ridges in Mars' southern high latitudes (70°-80°S, 56°W-6°E). Glacial eskers and inverted channels remain as active hypotheses for their formation [1,3-4,7-14]. A growing body of literature uses the esker interpretation as a basis for inferences about meltwater production (and, by extension, habitability) beneath a putative former ice sheet thought to have extended into the region of the DA during Mars' Hesperian period, despite a lack of rigorous quantitative testing of the esker hypothesis [e.g. 10-11,13,14].

Methods: We digitized DA ridge *segments* (individual, unbroken ridges) using ~115 and ~230 m/pixel MOLA DEMs and ~6 m/pixel CTX [15] and ~20 m/pixel HRSC [16] images. We conservatively grouped chains of related ridge segments, separated by gaps, into longer ridge *systems*. Standalone segments <10 km in length were excluded.

Plan view ridge geometry: We calculated system length (L_i) by linearly interpolating across gaps between segments. We calculated continuity as the ratio between the total length of segments comprising a system and L_i , and sinuosity as the ratio between L_i and the shortest linear distance between end points of the system.

Longitudinal change in ridge height and bed slope: We obtained Cross Sectional (CS) topographic profiles at ~1 km spacing (within the 115 m/pixel DEM) along four major ridges (A-D) and calculated the percentage down-ridge change in ridge height (dH). We used base elevations (average elevation of two base points on each CS profile) to calculate longitudinal bed slope (θ_L) between successive CS profiles. Calculations were not performed across ridge gaps or junctions.

Results and analysis: In total, we mapped ~7514 km of ridge systems (Fig. 1a, $n = 260$). Plan view geometry data for systems of the DA are displayed in Table 1. Maximum lengths are consistent with previous workers [7-8,10,13]. Gaps between segments account for ~10% of L_i . Some systems are more fragmented, with a minimum continuity of 0.59 ± 0.02 .

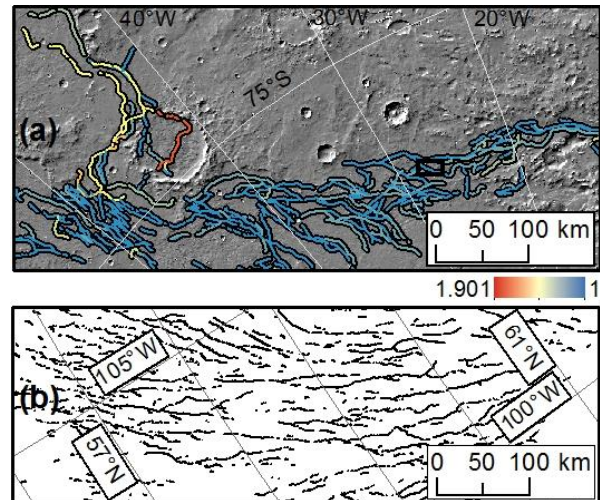


Figure 1. a) DA classified by system sinuosity. MOLA hillshade basemap. Black box delineates Fig. 3b. b) Map of a sample of Canadian eskers [2,17].

	Canada	Dorsa Argentea
Sample size, n	5932	260
Continuity	0.65	0.90
Mean length (km)	15.6	36.5
Median length (km)	4.1	22.2
Maximum length (km)	760	314
Mean sinuosity	1.08	1.10
Median sinuosity	1.06	1.07
Maximum sinuosity	2.45	1.91

Table 1. Plan view geometries of Dorsa Argentea and Canadian [2] esker systems.

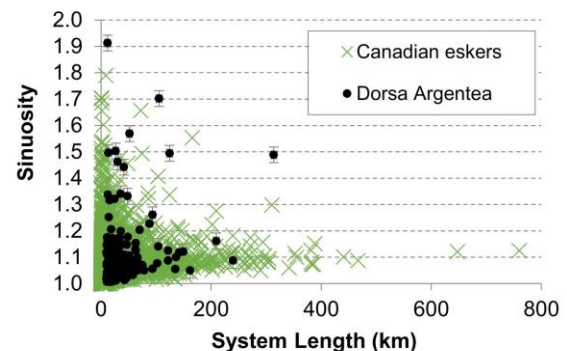


Figure 2. System sinuosity and length of the DA and Canadian eskers [2].

System sinuosity is consistent with values obtained by previous workers [8,13]. Long systems are typically straighter than shorter ones (Fig. 2) and those at the entry to East Argentea Planum have higher sinuosity ($\sim 1.48-1.7 \pm 0.03$) than those within the main valley ($\sim 1-1.3 \pm 0.03$, Fig. 1a).

We observe strong increases in ridge height on downhill slopes and decreases on uphill slopes (Fig. 3a) for ridges A (Fig. 3b) and B. Ordinary least squares regression analyses indicate that θ_L explains 51.68% ($p = 0.000$) and 39.37% ($p = 0.003$) of variance in dH on ridges A and B, respectively, confirming previously observed topographic relationships [3-4].

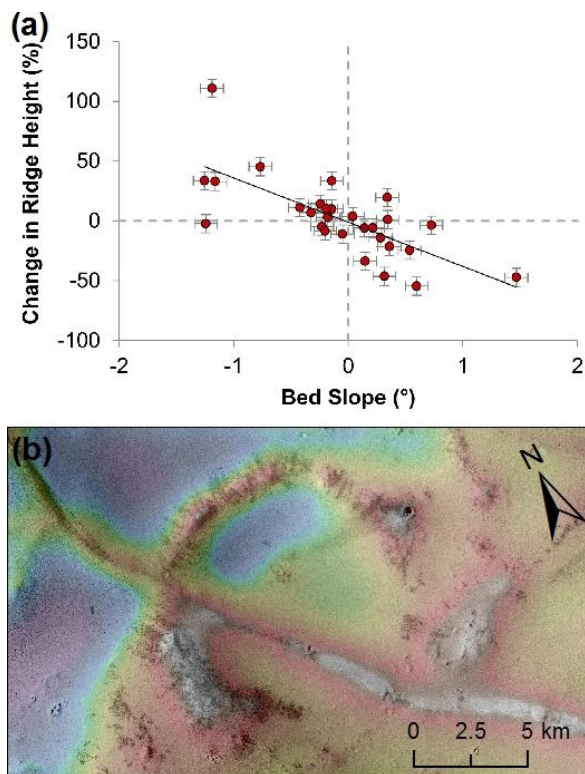


Figure 3. *a*) dH against θ_L for Ridge A. Positive values of θ_L are uphill and negative values downhill. *b*) A section of Ridge A passing through a crater. CTX images B12_014_285_1025_XN_77S026W and B12_014351_1024_XN_77S028W overlain by MOLA 512 ppd gridded topography. Extent shown in Fig. 1a.

Discussion: Plan view geometries of the DA are compared to >5900 Canadian esker systems (Fig. 1b) [2] in Table 1. The DA exhibit similar log-normal length distributions to the Canadian eskers. The great lengths and high continuity of the longest DA ridges, reconstructed ice surface slopes of $\sim 0.06^\circ$ [14], a putative paleolake in Argentea Planum [10] and fan-forms at ridge termini in this region [14] are consistent with terrestrial eskers formed synchronously in long, stable

channels extending from the interior of a former, likely stagnant, ice sheet and terminating in a proglacial lake [13,18]. The lower sinuosity of longer systems relative to shorter systems (Fig. 2) is consistent with the Canadian eskers. The consistently low sinuosity of ridges in the main basin supports their formation beneath thick ice, while higher sinuosity of the northernmost ridges supports their formation closer to a stable former ice margin. Variations in ridge height along ridges A (Fig. 3a) and B adhere to topographic relationships observed for terrestrial eskers arising from variations in energy available for melting of roofs of subglacial esker-forming conduits [5-6].

Conclusions: (1) Statistical distributions of length and sinuosity of the DA are similar to those of terrestrial eskers in Canada. (2) Plan view geometries of the DA support formation in conduits extending towards the interior of an ice sheet that thinned towards its northern margin, terminating in a proglacial lake. (3) Statistical tests for relationships between ridge height and topography similar to those explained by the physics of meltwater flow through subglacial meltwater conduits for terrestrial eskers, confirm the strength of these relationships for two of four major DA ridges.

Acknowledgements: FEGB is grateful for financial support from the British Society for Geomorphology and the Ogden Trust, and to RD Storrar for the terrestrial esker data in Figures 1 and 2.

References: [1] Butcher, F.E.G. et al. (2016) *Icarus*, In Review. [2] Storrar R.D. et al. (2014) *Quat. Sci. Rev.*, 105, 1-25. [3] Head J.W. and Hallet B. (2001) *LPSC XXXII*, Abstract #1366. [4] Head J.W. and Hallet B. (2001) *LPSC XXXII*, Abstract #1373. [5] Shreve R.L. (1972) *J. Glaciol.*, 11, 205-214. [6] Shreve R.L. (1985) *Geol. Soc. Am. Bull.*, 96, 639-646. [7] Howard, A.D. (1981) *NASA Tech. Memo.* 84211, 286-288. [8] Metzger, S.M. (1992) *LPSC XXIII*, Abstract #1448 [9] Tanaka K.L. and Kolb E.J. (2001) *Icarus* 154, 3-21 [10] Head, J.W. and Pratt, S. (2001) *J. Geophys. Res. Planets* 106, 12275-12299. [11] Ghatan G.J. and Head J.W. (2004) *J. Geophys. Res.* 109, E07006 [12] Tanaka K.L. et al. (2014) *USGS SIM* 3292. [13] Kress, A.M. and Head, J.W. (2015) *Planet. Space Sci.* 109-110, 1-20. [14] Scanlon K.E. and Head J.W. (2015) *LPSC XLVI*, Abstract #2247. [15] Malin, M.C. et al. (2007) *J. Geophys. Res.* 112, E05S04. [16] Neukum G. et al. (2004) *ESA Special Pub.* 1240, 17-35. [17] Storrar R.D. et al. (2013) *J. Maps* 9, 3, 456-473 [18] Brennand T.A. (2000) *Geomorphology* 32, 263-293. [19] Brennand T.A. (1994) *Sediment. Geol.* 91, 9-55.